Supporting Information

The Role of Oxygen Excess on Fluoride Intercalation in Ruddlesden–Popper Electrodes for Fluoride Ion Batteries: The Case of $LaSrMnO_4$

Gabriele Mezzadra[a], Xiangwei Guo [b], Marco Ravalli[a], Clemens Ritter[c], Davide Ceresoli[d], Oliver Clemens[b] and Cristina Tealdi[a]

[a] Department of Chemistry, University of Pavia, Via Taramelli 12, 27100, Pavia, Italy. E-mail: cristina.tealdi@unipv.it

[b] University of Stuttgart, Institute for Materials Science, Materials Synthesis Group, Heisenbergstraße 3, 70569 Stuttgart, Germany

[c] Institut Laue-Langevin, 71 Avenue des Martyrs, 38042 Grenoble, France

[d] Istituto di Scienze e Tecnologie Chimiche “Giulio Natta” (SCITEC) del Consiglio Nazionale delle Ricerche (CNR), via C. Golgi, 19, 20133 Milano, Italy

Table S1 Rietveld refined crystallographic parameters and agreement factors for $LaSrMnO_4$ at RT (a) and 150 °C(b); for $LaSrMnO_4F$ at RT (c), 150 °C (d) and 300 °C (e).

a) $LaSrMnO_4$ at RT, SG: *I4/mmm*. R_{wp}: 9.47 %

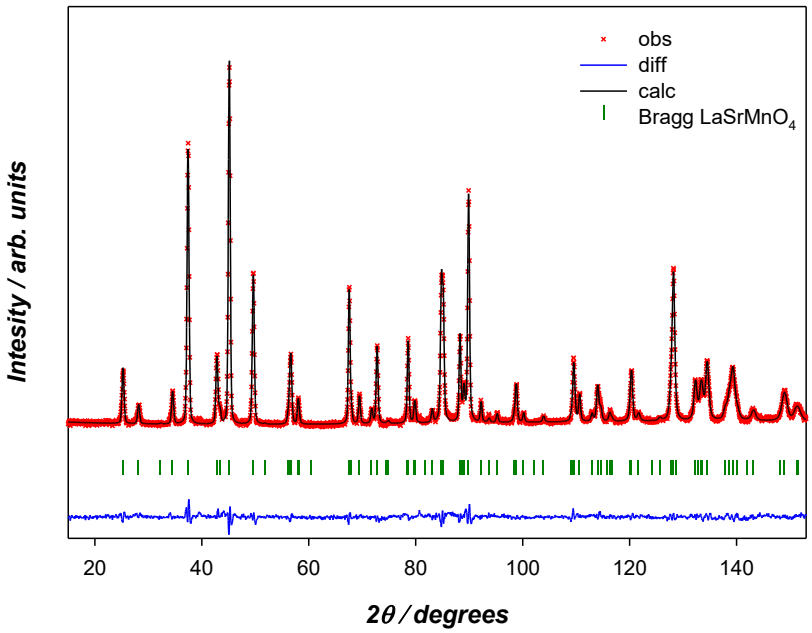

a (Å)	c (Å)	α=β=γ (°)	vol (Å^3)
3.80107(6)	13.1105(3)	90	189.421(7)

species	x	y	z	Occ	Beq
La	0.5	0.5	0.14351(9)	0.5	0.32(2)
Sr	0.5	0.5	0.14351(9)	0.5	0.32(2)
Mn	0	0	0	1	0.12(5)
O1	0.5	0	0	1	0.70(3)
O2	0	0	0.17184(11)	1	1.15(3)

b) $LaSrMnO_4$ at 150 °C, SG: *I4/mmm*. R_{wp}: 8.37 %

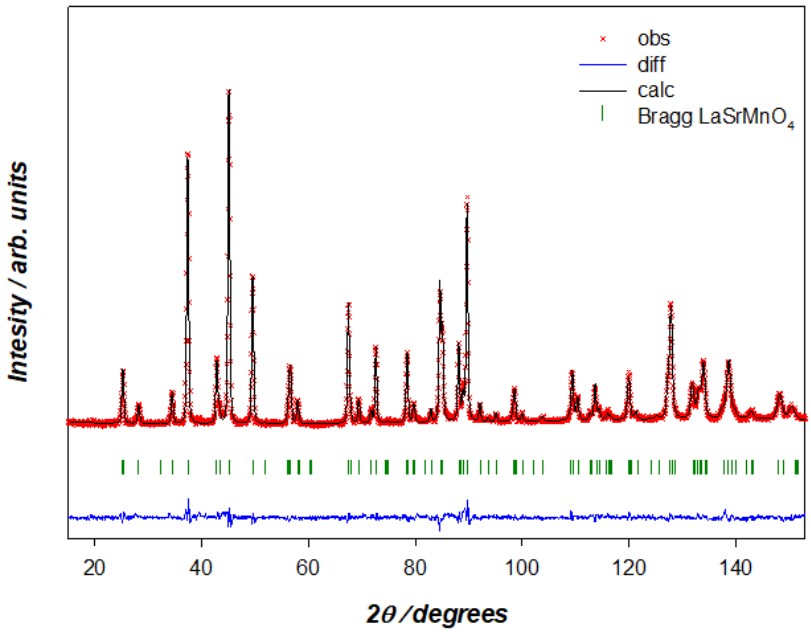

a (Å)	c (Å)	α=β=γ (°)	vol (Å^3)
3.80875(6)	13.1193(3)	90	190.316(7)

species	x	y	z	Occ	Beq
La	0.5	0.5	0.14353(9)	0.5	0.52(2)
Sr	0.5	0.5	0.14353(9)	0.5	0.52(2)
Mn	0	0	0	1	0.25(5)
O1	0.5	0	0	1	0.88(3)
O2	0	0	0.17173(11)	1	1.36(3)

c) $LaSrMnO_4F$ at RT. Ag SG: *Fm-3m*, $LaSrMnO_4$ SG: *I4/mmm*, $LaSrMnO_4F$ SG: *C2/m*, $LaSrMnO_4F_2$ SG: *I4/mmm*. R_{wp}: 9.88 %

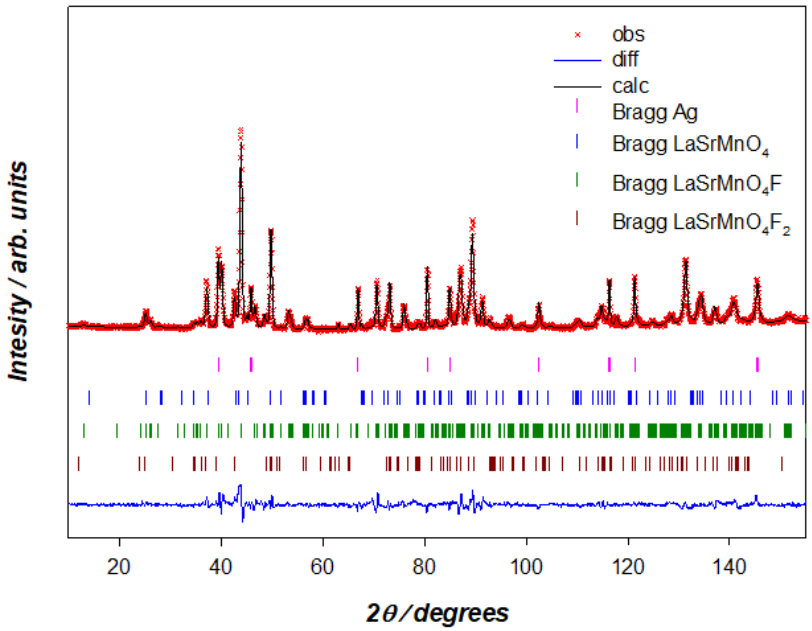

a (Å)	b (Å)	c (Å)	α=γ (°)	β (°)	vol (Å^3)
5.3562(5)	5.3489(4)	14.0935(11)	90	89.945(15)	403.78(6)

species	x	y	z	Occ	Beq
La1	0.7500	0.0000	0.0980(7)	0.5	0.57(17)
Sr1	0.7500	0.0000	0.0980(7)	0.5	0.57(17)
La2	0.7500	0.0000	0.3812(6)	0.5	0.67(17)
Sr2	0.7500	0.0000	0.3812(6)	0.5	0.67(17)
Mn	0.7330	0.0000	0.7726(8)	1	0.13(8)
O1	0.5000	0.2500	0.7764(5)	1	0.73(10)
O2	0.7500	0.0000	0.9230(7)	1	0.84(20)
O3	0.7500	0.0000	0.6449(7)	1	1.07(20)
F	0.0000	0.7500	0.5000	0.95(2)	1.52(18)

phase	Wt%
Ag	28.7(18)
LaSrMnO4	4.0(3)
LaSrMnO4F1	61.63(9)
LaSrMnO4F2	5.7(4)

d) $LaSrMnO_4F$ at 150 °C. Ag SG: *Fm-3m*, $LaSrMnO_4$ SG: *I4/mmm*, $LaSrMnO_4F$ SG: *C2/m*, $LaSrMnO_4F_2$ SG: *I4/mmm*. R_{wp}: 10.03 %

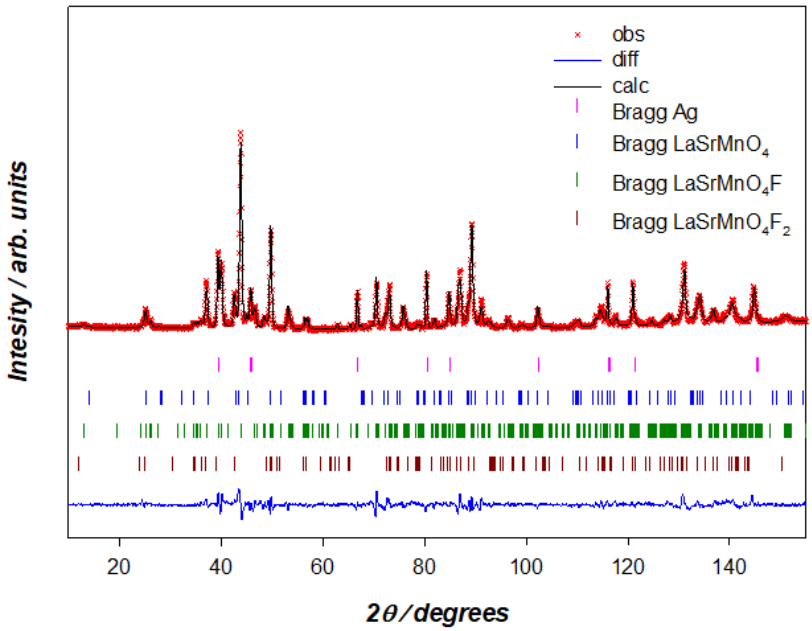

a (Å)	b (Å)	c (Å)	α=γ (°)	β (°)	vol (Å^3)
5.3552(3)	5.3630(6)	14.1183(14)	90	89.961(10)	405.36(6)

species	x	y	z	Occ	Beq
La1	0.7500	0.0000	0.0998(5)	0.5	0.64(10)
Sr1	0.7500	0.0000	0.0998(5)	0.5	0.64(10)
La2	0.7500	0.0000	0.3797(6)	0.5	0.71(13)
Sr2	0.7500	0.0000	0.3797(6)	0.5	0.71(13)
Mn	0.7500	0.0000	0.7696(7)	1	0.33(16)
O1	0.5000	0.2500	0.7776(5)	1	0.92(10)
O2	0.7500	0.0000	0.9270(7)	1	0.96(20)
O3	0.7500	0.0000	0.6413(7)	1	1.43(20)
F	0.0000	0.7500	0.5000	0.95(2)	1.64(17)

phase	Wt%
Ag	29.4(7)
LaSrMnO4	3.11(17)
LaSrMnO4F1	62.3(7)
LaSrMnO4F2	5.16(15)

e) $LaSrMnO_4F$ at 300 °C. Ag SG: *Fm-3m*, $LaSrMnO_4$ SG: *I4/mmm*, $LaSrMnO_4F$ SG:*C2/m*, $LaSrMnO_4F_2$ SG: *I4/mmm*. R_{wp}: 9.41 %

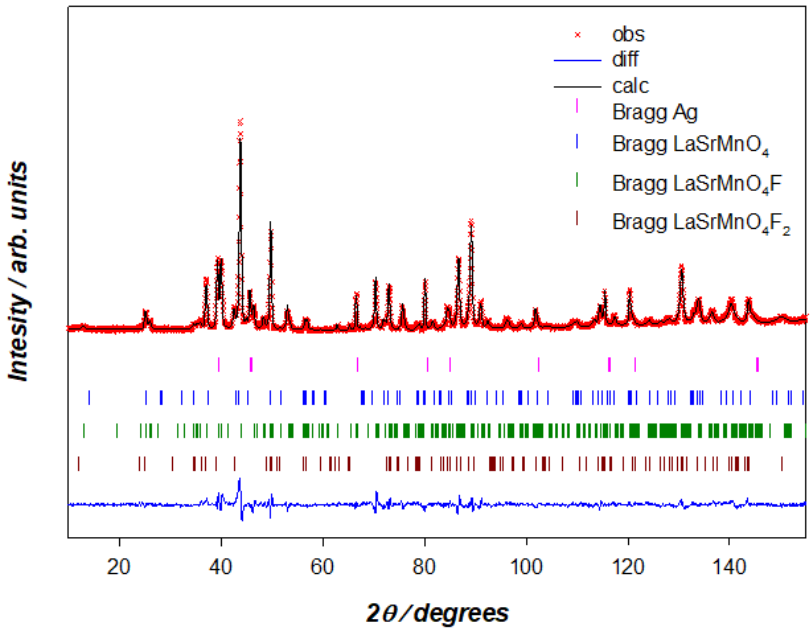

a (Å)	b (Å)	c (Å)	α=γ (°)	β (°)	vol (Å^3)
5.3665(5)	5.3576(3)	14.1781(10)	90	90.114(11)	407.64(6)

species	x	y	z	Occ	Beq
La1	0.7500	0.0000	0.1007(5)	0.5	0.51(10)
Sr1	0.7500	0.0000	0.1007(5)	0.5	0.51(10)
La2	0.7500	0.0000	0.3794(5)	0.5	0.89(13)
Sr2	0.7500	0.0000	0.3794(5)	0.5	0.89(13)
Mn	0.7500	0.0000	0.7689(6)	1	0.58(14)
O1	0.5000	0.2500	0.7780(4)	1	0.90(9)
O2	0.7500	0.0000	0.9269(6)	1	1.06(20)
O3	0.7500	0.0000	0.6414(6)	1	1.53(20)
F	0.0000	0.7500	0.5000	0.95(2)	1.76(16)

phase	Wt%
Ag	30.6(7)
LaSrMnO4	2.21(16)
LaSrMnO4F1	64.1(7)
LaSrMnO4F2	3.15(13)

Figure S1 Rietveld refinement of $LaSrMnO_4F$ at RT with tetragonal (*P4/nmm*) space group (a) and monoclinic (*C2/m*) space group (b). R_{wp} are respectively 11.31 % and 10.03 %.

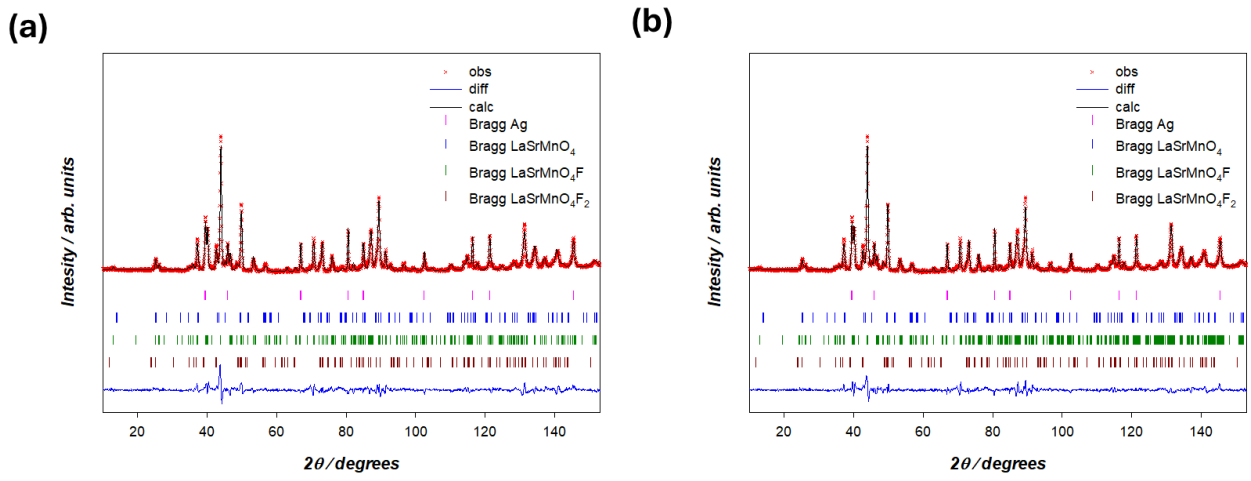

Figure S2 Manganese oxygen octahedra in the *P4/nmm* structure and *C2/m* structure. Three different angles are considered. The red one is between the two apical oxygen (O2 and O3), the yellow one between two equatorial oxygen and the black one between one apical (O2) and one equatorial oxygen. Important to note is the tilting between the two apical oxygen from 180° in the *P4/nmm* structure to 177.39° in the *C2/m* structure.

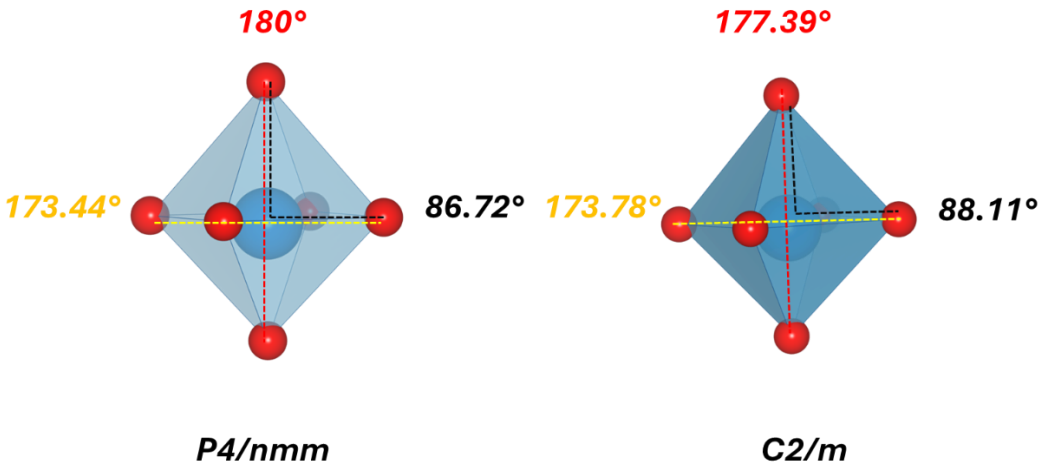

Figure S3 Fluoride-ion layers in the *P4/nmm* (a) and *C2/m* (b) structures. In the *P4/nmm* phase, the nearest-neighbor fluoride ions are aligned along the ⟨110⟩ direction, while in the *C2/m* structure they are oriented along the ⟨100⟩ direction.

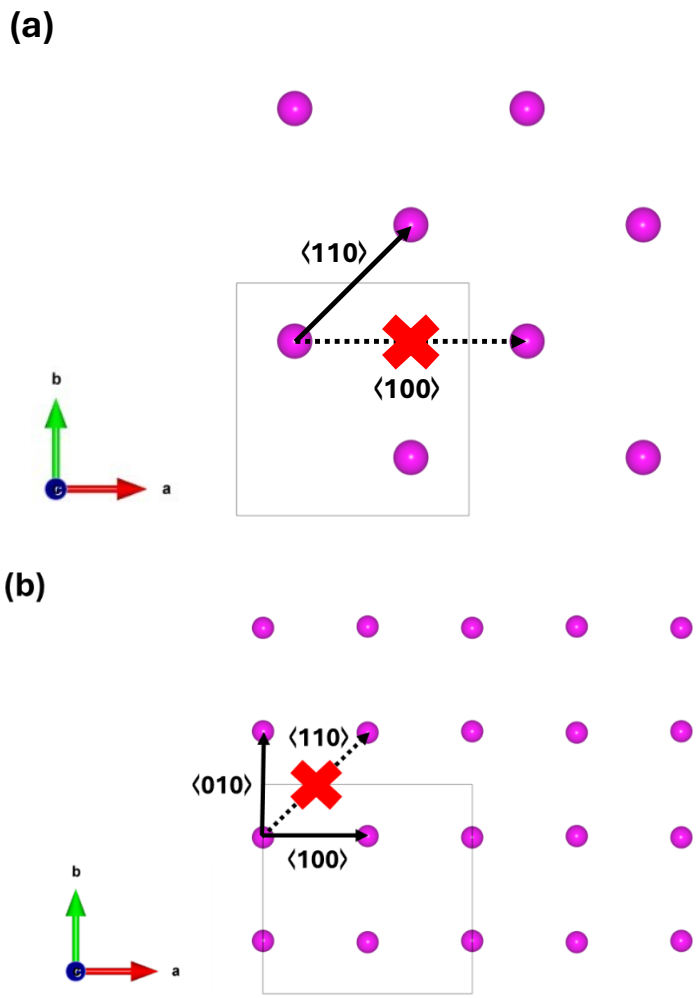

Table S2 Unit cell volume at different temperatures after the NPT simulations, a simulated thermal expansion coefficient of 59.7 × 10^{-6} K^{-1} was obtained for the $LaSrMnO_4F_{0.8}$ composition.

Temperature (K)	Unit Cell Volume (Å^3)
300	214.19
350	214.78
400	215.34
450	216.13
500	216.55
550	217.32
600	217.89
650	218.51
700	219.37

Figure S4 Mean squared displacement (MSD) at 700 K for *$LaSrMnO_4F_{0.8}$*. A zoom of the initial part of the simulation with fluoride ions omitted. Oxygen exhibits the highest vibrational motion among immobile species; manganese is the least mobile, and strontium and lanthanum show similar displacements.